arXiv:1412.4666v1 [cond-mat.quant-gas] 1 Dec 2014

Probing Sound Speed of an Optically-Trapped Bose Gas with Periodically Modulated Interactions by Bragg Spectroscopy

Lei Chen,[1] Wu Li,[1] Zhu Chen,[2] Zhidong Zhang,[1] and Zhaoxin Liang[1,*]

[1] *Shenyang National Laboratory for Materials Science, Institute of Metal Research, Chinese Academy of Sciences, Wenhua Road 72, Shenyang 110016, China*
[2] *National Key Laboratory of Science and Technology on Computational Physics, Institute of Applied Physics and Computational Mathematics, Beijing 100088, China*

A Bose-Einstein condensate (BEC) with periodically modulated interactions (PMI) has emerged as a novel kind of periodic superfluid, which has been recently experimentally created using optical Feshbach resonance. In this paper, we are motivated to investigate the superfluidity of a BEC with PMI trapped in an optical lattice (OL). In particular, we explore the effects of PMI on the sound speed and the dynamical structure factor of the model system. Our numerical results, combined with the analytical results in both the weak-potential limit and the tight-binding limit, have shown that the PMI can strongly modify the sound speed of a BEC. Moreover, we have shown that the effects of PMI on sound speed can be experimentally probed via the dynamic structure factor, where the excitation strength toward the first Bogoliubov band exhibits marked difference from the non-PMI one. Our predictions of the effects of PMI on the sound speed can be tested using the Bragg spectroscopy.

PACS numbers: 37.10.Jk, 67.85.Hj, 42.50.-p

* Corresponding author: zhxliang@imr.ac.cn

I. INTRODUCTION

By using the optical Feshbach resonance (OFR), a Bose-Einstein condensate (BEC) with periodically modulated interactions (PMI) has been recently realized in the experiments [1–4]. Such a novel periodic superfluid, which has no analogue in condensed matter physics, has opened up new avenues to exploring the superfluidity of quantum many-body systems with PMI.

Meanwhile, there exists another conventional way of creating a periodic superfluid via loading a BEC into an optical lattice (OL) [5–14]. Both being periodic, however, a BEC with PMI and an optically trapped BEC have exhibited interestingly different superfluid behavior. For example, it's well known that the dynamic instability plays a key role in destroying the superfluidity in a periodic superfluid [15–23]. In this context, Ref. [24] has found that, in a BEC with PMI, all Bloch waves in the lowest band will inevitably become dynamical unstable when the PMI is strong enough; whereas in comparison, an optically trapped BEC in the lowest band will be more stable with increasing interaction. Inspired by such comparisons, we are interested in the case when a BEC is in the presence of both PMI and an optical lattice. Here we investigate the effect of PMI on the sound speed of an optically trapped BEC, and discuss its exploration via measuring the dynamic structure factor using the Bragg spectroscopy [25–31]. The motivation is twofold. First, the sound speed is intimately related to the concept of superfluidity and its exploration. Second, the application of Bragg spectroscopy in such a novel kind of periodic superfluid is itself worthy of more efforts.

The main purpose of this work is to theoretically investigate both the sound speed and the dynamical structure factor of a BEC with PMI trapped in an OL [32, 33] using the mean-field theory. Our results show that, compared to the non-PMI counterpart, (i) the PMI can significantly affect the sound speed; (ii) the excitation strength toward the first Bogoliubov band in a BEC with PMI is markedly difference from the non-PMI one. Based on these calculations, we also discuss the conditions for possible experimental realizations of our scenarios.

The paper is organized as follows. First, in Sec. II we derive the effective model for a quasi-one-dimensional BEC with PMI in an OL. Then in Sec. III, we study the sound propagation and dynamic structure factor of the model system in different parameter regimes, using both analytical and numerical approaches. Finally, we summarize our results in Sec. IV and present an outlook.

II. THE MODEL SYSTEM

We consider a BEC with PMI by OFR trapped in a strongly anisotropic lattice potential as shown in Fig. 1. Specifically, the transverse lattice confinement is tuned sufficiently strong to freeze the atomic motion in these directions such that atoms are only allowed to tunnel in the x-direction, leading to the realization of a quasi-one-dimensional geometry [34, 35]. The OL along the x-direction reads $V\cos(2k_Lx)$ with V being the lattice strength. The wave vector of the lattice $k_L = 2\pi\sin(\theta_L/2)/\lambda_L$ can be manipulated via the wavelength of the lasers λ_L and the angle θ_L between the two lasers. The PMI in the form of $g_1 + g_2\cos(2k_Zx)$ for a BEC has been experimentally realized using OFR. Here, g_1 and g_2 are positive parameters and $k_Z = 2\pi\sin(\theta_R/2)/\lambda_Z$ with λ_Z being the wavelength of the OFR and θ_R being the angle between the OFR beams (see Fig. 1). Note that g_1, g_2 and k_Z can all be tuned experimentally by adjusting OFR laser beams. At the mean-field level, our model system can be well described by the Gross-Pitaevskii (GP) Eq. [24],

$$i\hbar\frac{\partial\psi}{\partial t} = -\frac{\hbar^2}{2m}\frac{\partial^2}{\partial x^2}\psi + V\cos(2k_Lx)\psi + [g_1n_0 + g_2n_0\cos(2k_Zx)]|\psi|^2\psi, \tag{2.1}$$

where m is the atom mass, ψ is the condensate wave function and n_0 is the average condensate density. While both k_L and k_Z can be tuned, as a first step to investigating the superfluidity of the novel periodic superfluid under consideration, we will limit ourselves to the case $k_L = k_z$ throughout this paper. The corresponding 1D GP Eq. (2.1) reads in a dimensionless form as

$$i\hbar\frac{\partial\psi}{\partial t} = -\frac{1}{2}\frac{\partial^2}{\partial x^2}\psi(x) + v\cos(x)\psi(x) + [c_1 + c_2\cos(x)]|\psi(x)|^2\psi(x). \tag{2.2}$$

In Eq. (2.2), the energy unit is $8E_R$ with $E_R = 2\hbar^2\pi^2/m\lambda_L^2$ being the recoil energy and the length unit is $1/2k_L$. The lattice strength and nonlinear coefficients scale as: $v = V/(8E_R)$, $c_1 = g_1n_0/(8E_R)$ and $c_2 = g_2n_0/(8E_R)$.

In this work, we are interested in (i) the sound speed in the novel periodic superfluid described by Eq. (2.2); (ii) the probe of sound speed by using the Bragg spectroscopy, where the dynamic structure factor of the model system is directly measured. Before we proceed into concrete calculations, let us first present a general framework concerning the sound speed and the dynamic structure factor of the system under consideration:

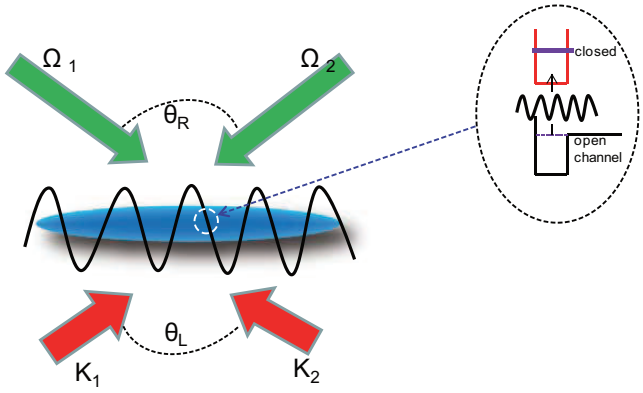

FIG. 1. (Color online) Schematic setup of a BEC with PMI in an OL. Two laser beams of Ω_1 and Ω_1 generate the periodically modulated interaction by OFR; while the other two beams of k_1 and k_2 generate the OL.

(i) It has been known that the sound propagation and its speed of an optically trapped BEC can be discussed from two perspectives [36]. In one, the sound speed is viewed as a quantity intimately related to the superfluidity of a BEC and its macroscopic dynamics, the definition [36–38]

$$c_s = \sqrt{\frac{1}{\kappa m^*}}, \tag{2.3}$$

with the compressibility κ and the effective mass m^* being defined as follows,

$$\frac{1}{m^*} = \lim_{k\to 0}\frac{d^2\epsilon_k}{dk^2}, \qquad \kappa^{-1} = n_0\frac{\partial\mu}{\partial n_0}. \tag{2.4}$$

Here, the chemical potential μ reads $\mu = \partial(n_0\epsilon_k)/\partial n_0$ with the energy per particle ϵ_k being written as,

$$\epsilon_k = \frac{1}{2\pi}\int_{-\pi}^{\pi} dx\left[\frac{1}{2}\left|\frac{\partial\psi}{\partial x}\right|^2 + v\cos(x)|\psi|^2 + \frac{1}{2}\left(c_1 + c_2\cos(x)\right)|\psi|^4\right]. \tag{2.5}$$

On the other hand, the sound propagation in a BEC can be also treated as a long wavelength response to an external perturbation, and the corresponding speed can be calculated using Bogoliubov theory. In more details, the low-energy excitation in connection to the sound propagation can be described by a small perturbation to the wave function in Eq. (2.2) as $\psi(x,t) = [\psi_0(x) + \delta\psi(x,t)]\exp(-i\mu t)$, with ψ_0 being the ground state. By decomposing $\delta\psi(x,t) = u(x)\exp(iqx - i\omega t) + v^*(x)\exp(-iqx + i\omega t)$, together with Eq. (2.2), we obtain Bogoliubov-de Gennes (BdG) equations reading

$$\begin{aligned}
&\left[-\frac{1}{2}\frac{\partial^2}{\partial x^2} + v\cos(x) - \mu + 2\left(c_1 + c_2\cos(x)\right)|\psi|^2\right]u_{jq} + \left(c_1 + c_2\cos(x)\psi^2\right)v_{jq} = \omega_j(q)u_{jq}\\
&\left[-\frac{1}{2}\frac{\partial^2}{\partial x^2} + v\cos(x) - \mu + 2\left(c_1 + c_2\cos(x)\right)|\psi|^2\right]v_{jq} + \left(c_1 + c_2\cos(x)\psi^{*2}\right)u_{jq} = -\omega_j(q)v_{jq}.
\end{aligned} \tag{2.6}$$

Here, u and v are the Bogoliubov amplitudes that satisfy the normalization and orthogonality conditions $\int\left[u^*_{j'q}(x)u_{jq}(x) - v^*_{j'q}(x)\right.$ $\delta_{j',j}$; the q and $\omega_j(q)$ are the wave vector and the energy of the Bogoliubov excitations with j being the band index, respectively. According to Eq. (2.6), the sound speed of a quasi-1D BEC under consideration can then be defined as

$$c_s = \lim_{q\to 0}\frac{\omega_{j=1}(q)}{q}. \tag{2.7}$$

These two definitions on the sound speed (Eqs. (2.7), (2.3)) have been proved equivalent [36] for an optically trapped BEC.

(ii) In the second scenario, the Bragg spectroscopy measures the energy spectrum of the model system by stimulating small-angle light scattering, delivering a momentum p and an energy ω. Theoretically, such light scattering directly corresponds to the dynamic structure factor of $S(p,\omega)$, which is the Fourier transform of density-density correlations

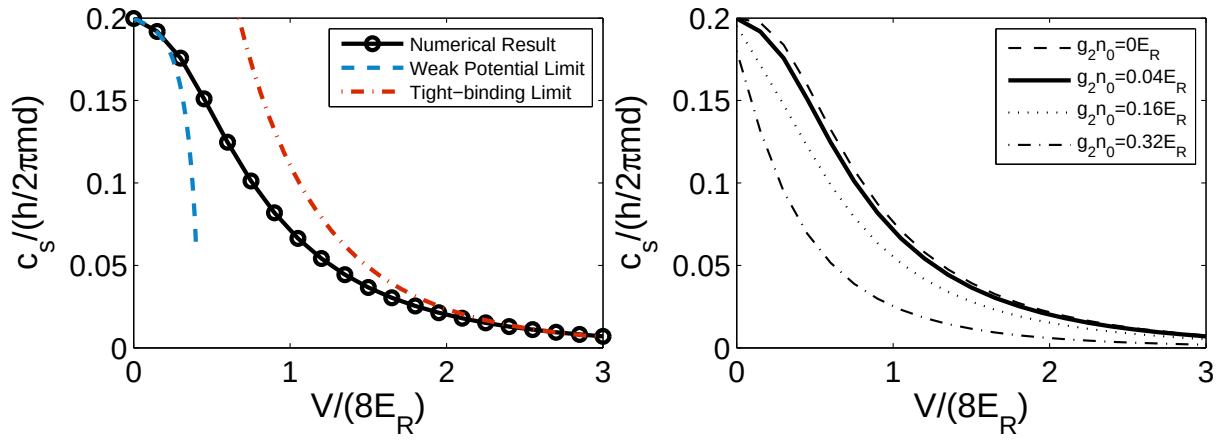

FIG. 2. (Color online) Left panel: Sound speed of a BEC with PMI trapped in an OL as a function of the lattice depth V with $g_1 n_0 = 0.32E_R$ and $g_2 n_0 = 0.04E_R$. The solid, dashed and dot-dashed lines correspond to the numerical results, the analytical results in weak-potential limit and tight-binding limit respectively. Right panel: The effects of $g_2 n_0$ on the sound speed via lattice strength V with fixed $g_1 n_0 = 0.32E_R$.

function of the system. For a periodic superfluid, there exist an infinite set of ω_j for each q in the first Brillouin zone, forming a Bogoliubov band labeled by index j. Hence, when the external probe p is varied, an infinite set of excitation strength $Z_j(p)$ relative to the j-th Bogoliubov band are excited, reading,

$$Z_j(p) = \left| \int \left[u_{jq}^* + v_{jq}^* \right] e^{ipx} \psi_0(x) dx \right|^2 , \tag{2.8}$$

where q lies in the first Brillouin zone and is fixed by the relation $q = p + l2\pi/d$. Summing up all the $Z_j(p)$ in Eq. (2.8) under the condition of energy conservation, we obtain the dynamic structure factor as follows,

$$S(p, \omega) = \sum_j Z_j(p) \delta(\omega - \omega_j(p)), \tag{2.9}$$

The sound speed of a BEC can be extracted directly from the slope of the linear part of the excitation spectrum by employing the Bragg spectroscopy. In more details, the Bragg spectroscopy in an optically-trapped BEC is performed by superimposing a periodic traveling wave potential on the lattice. Then, the technique of Bragg spectroscopy to measure the energy spectrum essentially boils down to probing the dynamic structure factor, namely the response of a BEC to an external density perturbation [25–31, 41].

Having laid out the basic theoretical framework, below we proceed to illustrate with an experimentally relevant system for concrete investigations. At mean field level, Eq. (2.2) describes a BEC with PMI in an OL, where the main physics is determined by three parameters, v, c_1 and c_2 (respectively characterize the lattice strength, the bare interaction strength, and the periodic interaction strength). All these parameters can be experimentally controlled using the state-of-art technologies. In typical experiments, the lattice strength V can be turned from 0 to $32E_R$ almost at will, corresponding to the regime of $0 \leq v \leq 4$. Furthermore, both the c_1 and c_2 can be controlled in a very versatile manner via the technology of OFR.

III. PROBING SOUND SPEED BY DYNAMIC STRUCTURE FACTOR

A. Sound speed

The previous section has set the stage for our study on the sound in a BEC with PMI trapped in an OL. In this section, we will systematically study the effects of PMI on the sound speed, using both analytical and numerical methods. As we have discussed in Eqs. (2.3) and (2.7), there exist two routes to calculating the sound speed. Note that Both approaches consists in numerically solving the GP Eq. (2.2) based on the Bloch theorem. Once the Bloch waves of ψ have been found, we can (i) proceed to numerically solve BdG Eq. (2.6) and then obtain the numerical

results of sound speed according to Eq. (2.3); or we can (ii) calculate the energy $E(k)$ from Eq. (2.5), derive the compressibility κ and the effective mass m^*, which will give the sound velocity c_s following from Eq. (2.7). In this work, we shall use both methods to calculate the sound speed, which will be shown to agree with each other as expected. Moreover, in order to comprehensively reveal the effects of PMI on the sound speed, we will proceed our analysis in two steps:

(i) In the first step, we fix the PMI of $g_2 n_0$, so as to figure out how the sound speed c_s responds to the variation of V. As shown in Fig. 2, with the increase of V, the sound speed c_s decreases monotonically, implying that the increasing effective mass m^* always wins the competition against the decreasing compressibility κ in determining c_s. In order to achieve a clearer understanding of Fig. 2, we have obtained analytical results in both the weak-potential limit and tight-binding limit. In the weak-potential limit, the analytical expression of sound speed are given by (see Eq. (A8) in Appendix)

$$c_s = \sqrt{c_1}\left[1 - \frac{c_2^2}{c_1\left(1+4c_1\right)} - \frac{c_2^2 - v^2}{c_1\left(1+4c_1\right)^2} - \frac{\left(c_2+v\right)^2}{c_1\left(1+4c_1\right)^3} - \frac{4\left(c_2+v\right)^2}{\left(1+4c_1\right)^2}\right]. \tag{3.1}$$

It's clear that if $c_2 = 0$, Eq. (3.1) recovers the sound speed in an OL [36, 39, 40] which decreases monotonically with v as it should be. In the presence of PMI with $c_2 \neq 0$, the second term and the last two terms in the square brackets in Eq. (A8) are definitely negative, whereas the third term can be either positive or negative depending on the c_2 relative to v. This suggests that both c_2 and v play the same role in determining the c_s. Moreover, as is shown by the dashed curve in Fig. 2, our numerical results agree well with Eq. (3.1). In the opposite tight-binding limit, the analytically derived sound speed (see Eq. (A12) in the Appendix) also agrees well with the numerical result.

(ii) In the second step, we fix $g_1 n_0$ and scan the sound speed c_s as a function of V for different choices of $g_2 n_0$. As shown in the right panel in Fig. 2, the sound speed behaves very differently from the non-PMI one. Our results imply that the effect of PMI on the sound speed can be measured within the current experimental capabilities. In what follows, we will develop a scheme of probing the effects of PMI on the sound speed via the dynamic structure factor (DSF).

B. Dynamic Structure factor

In order to characterize and investigate the capability of measuring the sound speed by using the Bragg spectroscopy, we numerically calculate the DSF of the system defined in Eq. (2.9).

Before any further concrete calculations, we use the sum rule approach to analyze the basic properties of the dynamic structure factor. The first sum rule gives the static structure factor $S(p)$ by integrating the $S(p,\omega)$ [37, 38]

$$S(p) = \int S(p,\omega)d\omega = \sum_n Z_n(p,\omega). \tag{3.2}$$

We expect that $S(p)$ will be strongly affected by the combined presence of OL and PMI. The second f-sum rule on $S(p,\omega)$ is a direct consequence of particle conservation of the model system and represents a statement of the conservation law, reading [37, 38],

$$\int \hbar\omega S(p,\omega)d\omega = \frac{p^2}{2m}. \tag{3.3}$$

In the long wavelength limit, the static response function manifests itself as the response of the system density to a static force, which is intimately related to the compressibility of the system, giving the third sum rule [37, 38],

$$\lim_{p\to 0}\int \frac{S(p,\omega)}{\hbar\omega}d\omega = \frac{\kappa}{2}. \tag{3.4}$$

We emphasize that our following numerical results have been double-checked by checking whether they satisfy the above three sum rules.

Now, we are equipped to study the effects of PMI on the sound speed by calculating the $S(p,\omega)$. To this end, we shall focus on two scenarios: first, we set $g_2 n_0 = 0$ and calculate the dynamic structure factor, which will then serve as the reference for later comparisons. Then, we turn on the PMI ($g_2 n_0 \neq 0$) and study the effect of the combined presence of PMI and optical lattice on the dynamic and static structure factor.

In the first scenario where the PMI is absent ($g_2 n_0 = 0$), both the $S(p,\omega)$ and $S(p)$ are plotted in bold curves in Figs. 3, 4 and 5. In this case, we have recovered the main conclusions of a BEC in an OL, i.e. the excitations strength

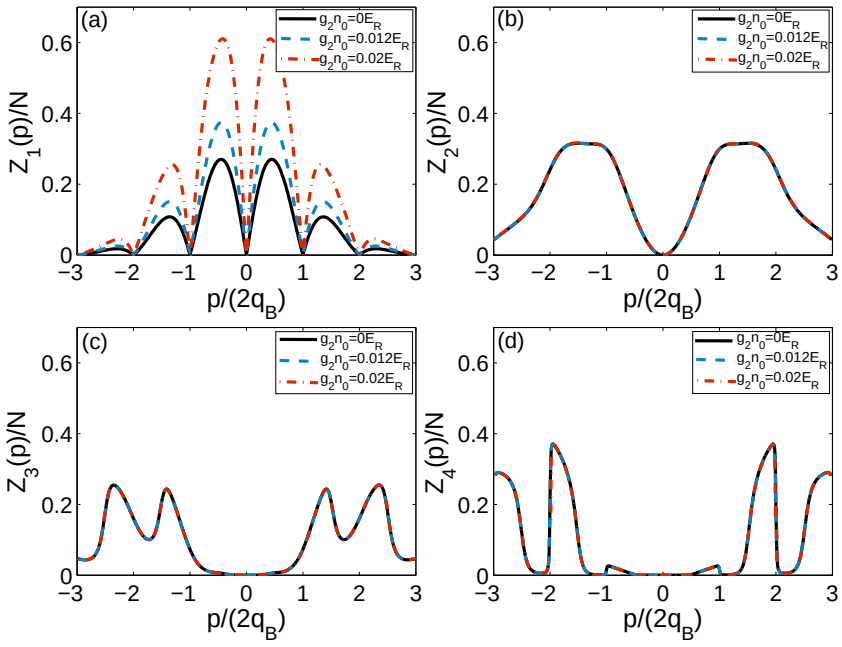

FIG. 3. (Color online) The excitation strengths Z_j $(j = 1, 2, 3, 4)$, as of function of momenta of an extra probe. The full, the dashed and the dot-dashed lines corresponds to $g_2n_0 = 0E_R$, $g_2n_0 = 0.012E_R$ and $g_2n_0 = 0.02E_R$ with $V = 10E_R$ and $g_1n_0 = 0.02E_R$, respectively.

Z_j $(j = 1, 2, 3, 4)$ toward the j-th Bogoliubov band develops the typical oscillating behavior as a function of p and vanishes at even multiples of the Bragg momentum because of phononic correlations.

In the second scenario, in which the PMI is turned on $(g_2n_0 \neq 0)$, the calculated lowest excitation strength Z_1 shows marked difference from the non-PMI one, as can be clearly seen from Figs. 3(a) and 4(a). In particular, with the increase of g_2n_0, the developed maximum values of Z_1 at the first Brillouin zone are greatly enhanced. In contrast, the effects of PMI are less pronounced for higher excitation strength Z_j $(j = 2, 3, 4)$ (see Figs. 3b, c, d and 4b, c, d). Summing up all the Z_j, we obtain the static structure factor (see Fig. 5). It follows from Fig 5 that, when the g_1n_0 is fixed, even a small $g_2n_0 \neq 0$ will lead to an observable modification of the static dynamic structure factor.

There are two qualitative ways to understand why the g_2n_0 has an important role in determining the maximum value of the Z_1 at the first Brillouin zone. First, this strong dependence can be explained in terms of the effective interaction $H_{int} = \int_{-\pi}^{\pi}(c_1+c_2\cos(x))|\psi|^4dx$ seen by each atom. The effective interaction is reduced with the increasing g_2n_0 as emphasized in Ref. [24]. Consequently, the reduced effective interatomic interaction makes the condensate more compressible, leading to an increase of maximum value of the Z_1 at the first Brillouin zone. Second, following the analysis in Ref. [33], the maximum value of Z_1 close to the edge of the first Brillouin zone can be approximately as $Z_1(q_B) \sim \sqrt{\kappa\delta/(\kappa\delta+1)}$ with $\delta = 2mE_R/\pi^2m^*$. This simple expression shows that Z_1 is quenched both by decreasing compressibility $(\kappa \to 0)$ and by increasing the effective mass $(\delta \to 0)$. Whether such a physical picture can be applied to our case is checked as follows. We choose to fix both g_1n_0 and g_2n_0 and plot the solid curves in Figs. 3a and 4a, corresponding to $V = 10E_R$ and $V = 5E_R$ respectively. The maximum of Z_1 is increased as expected by reducing the lattice depth V. Furthermore, we can obtain the analytical expressions of the κ and m^* as follows (see Eqs. (A6) and (A7) in Appendix),

$$\frac{1}{\kappa} = c_1 - \frac{2c_2^2}{1+4c_1} - \frac{2\left(c_2^2-v^2\right)}{\left(1+4c_1\right)^2} - \frac{2\left(c_2+v\right)^2}{\left(1+4c_1\right)^3} \tag{3.5}$$

and

$$\frac{1}{m^*} = 1 - \frac{8\left(c_2+v\right)^2}{\left(1+4c_1\right)^2} \tag{3.6}$$

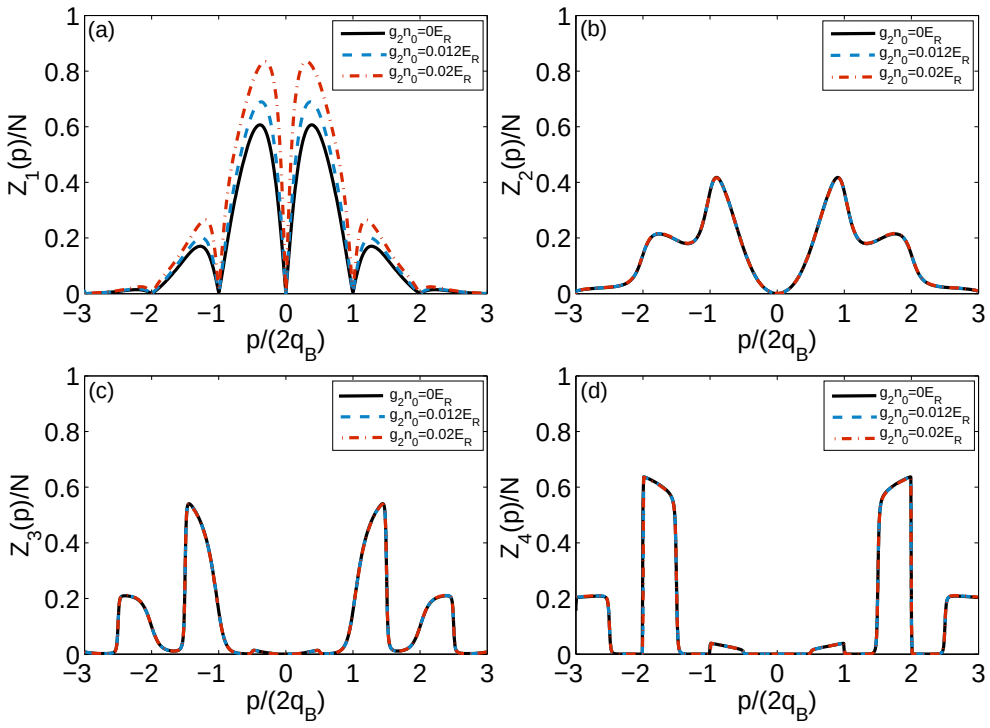

FIG. 4. (Color online) The excitation strengths Z_j $(j = 1, 2, 3, 4)$, as of function of momenta of an extra probe. The full, the dashed and the dot-dashed lines corresponds to $g_2n_0 = 0E_R$, $g_2n_0 = 0.012E_R$ and $g_2n_0 = 0.02E_R$ with $V = 5E_R$ and $g_1n_0 = 0.02E_R$, respectively.

It's clear from Eqs. (3.5) and (3.6) that Z_1 is increased by the competition of both increasing κ and m^* when g_2n_0 increases.

Moreover, the behavior of $S(p)$ at small momenta in Fig. 5 can be described exactly using the sum rule approach in Eq. (3.4). As shown in Ref. [33], the low p behavior of the $S(p)$ can be described by

$$\lim_{p\to 0} S(p) \sim \frac{|p|}{2\sqrt{c_1}}\left(1+\frac{c_2^2}{c_1\left(1+4c_1\right)}+\frac{\left(c_2^2-v^2\right)}{c_1\left(1+4c_1\right)^2}-\frac{4\left(c_2+v\right)}{\left(1+4c_1\right)^2}+\frac{\left(c_2+v\right)}{c_1\left(1+4c_1\right)^3}\right). \tag{3.7}$$

From this, we again conclude that the increase of g_2n_0 enhances the value of the static structure factor at low values of p, as clearly shown in Fig. 5.

IV. EXPERIMENTAL PERSPECTIVE AND CONCLUSION

Summarizing, we have studied the effects of PMI on both the sound speed and the dynamical structure factor of a BEC with PMI in an OL. Our results of sound speed show that the PMI can strongly influence the sound speed of BEC. Such effects of PMI can be probed experimentally by using the Bragg spectroscopy, which directly measures the dynamic structure factor of the system.

ACKNOWLEDGMENTS

We thank Ying Hu and Biao Wu for helpful and motivating discussions. This work is supported by the NSF of China (grant nos. 11004200 and 11274315).

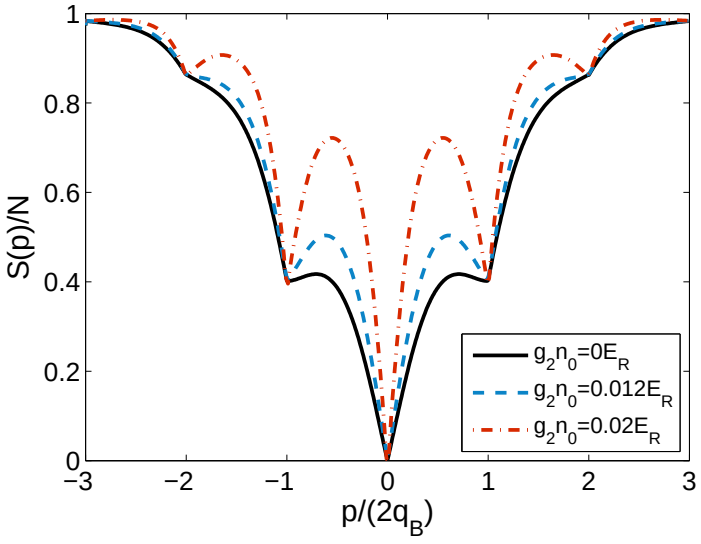

FIG. 5. (Color online) Static structure factor as a function of momenta of an extra probe. The solid, the dashed and the dot-dashed lines correspond to $g_2 n_0 = 0E_R$, $g_2 n_0 = 0.012E_R$ and $g_2 n_0 = 0.02E_R$ with $V = 10E_R$ and $g_1 n_0 = 0.02E_R$, respectively.

Appendix A: Sound velocity of a BEC with PMI in an OL: perturbation approach

1. Weak-potential regime

In the weak potential and interaction regime where $v \sim c_2 \sim \lambda$ (λ is a small parameter), both the OL potential (v) and PMI (c_2) can be treated as a perturbation to an unperturbed system consisting of a homogeneous qusi-1D BEC. For the considered case in our work where PMI has the same period with OL, we could develop a perturbation theory through the expansion of the condensate wave function $\psi(x)$ up to second order of the small parameters, i.e.

$$\psi(x) = \psi^{(0)}(x) + \lambda\psi^{(1)}(x) + \lambda^2\psi^{(2)}(x) + o(\lambda^3) \tag{A1}$$

Following the standard procedure [36], we calculate the condensate wave function and the chemical potential order by order, and the results are

$$\begin{aligned}\psi(x) = &\sqrt{n_0} \\ &-\frac{\sqrt{n_0}(V+g_2n_0)}{1-4k^2+4g_1n_0}\left((1-2k)e^{ix}+(1+2k)e^{-ix}\right) \\ &+\left(A\frac{2-2k+g_1n_0}{4-4k^2+4g_1n_0}-B\frac{g_1n_0}{4-4k^2+4g_1n_0}\right)e^{i2x} \\ &+\left(-A\frac{g_1n_0}{4-4k^2+4g_1n_0}+B\frac{2+2k+g_1n_0}{4-4k^2+4g_1n_0}\right)e^{-i2x}\end{aligned} \tag{A2}$$

and

$$\mu = \frac{1}{2}k^2 + g_1n_0 - \frac{(V+g_2n_0)(V+3g_2n_0)}{1-4k^2+4g_1n_0} + 2g_1n_0\frac{(3+4k^2)(V+g_2n_0)^2}{(1-4k^2+4g_1n_0)^2} \tag{A3}$$

with

$$A = \frac{n_0^{1/2}V}{2}\frac{(1-2k)(V+g_2n_0)}{1-4k^2+4g_1n_0} - \frac{n_0^{3/2}g_1(1-2k)(3+2k)(V+g_2n_0)^2}{(1-4k^2+4g_1n_0)^2} + \frac{n_0^{3/2}g_2}{2}\frac{(3-2k)(V+g_2n_0)}{1-4k^2+4g_1n_0} \tag{A4}$$

$$B = \frac{n_0^{1/2}V}{2}\frac{(1+2k)(V+g_2n_0)}{1-4k^2+4g_1n_0} - \frac{n_0^{3/2}g_1(1+2k)(3-2k)(V+g_2n_0)^2}{(1-4k^2+4g_1n_0)^2} + \frac{n_0^{3/2}g_2}{2}\frac{(3+2k)(V+g_2n_0)}{1-4k^2+4g_1n_0} \tag{A5}$$

Furthermore, we proceed to derive the energy of the BEC, and then calculate the effective mass m^* and the compressibility κ, respectively. The results are as follow,

$$\frac{1}{\kappa}=c_1-\frac{2c_2^2}{1+4c_1}-\frac{2\left(c_2^2-v^2\right)}{\left(1+4c_1\right)^2}-\frac{2\left(c_2+v\right)^2}{\left(1+4c_1\right)^3}+o\left(3\right) \tag{A6}$$

and

$$\frac{1}{m^*}=1-\frac{8\left(c_2+v\right)^2}{\left(1+4c_1\right)^2}+o\left(3\right) \tag{A7}$$

It thus follows from Eqs. (A6) and (A7) that the sound speed is derived as

$$c_s=\sqrt{c_1}\left[1-\frac{c_2^2}{c_1\left(1+4c_1\right)}-\frac{c_2^2-v^2}{c_1\left(1+4c_1\right)^2}-\frac{\left(c_2+v\right)^2}{c_1\left(1+4c_1\right)^3}-\frac{4\left(c_2+v\right)^2}{\left(1+4c_1\right)^2}\right] \tag{A8}$$

2. Tight-binding regime

We now turn to the tight-binding regime where $v\gg c_2$ (while the system is still kept in the superfluid regime). We can write the condensate wave function $\psi\left(x\right)$ as

$$\psi\left(x\right)=e^{ikx}\sum_L e^{ikL}f\left(x-L\right) \tag{A9}$$

where L denotes the position of different unit cells and f denotes the Wannier functions. Having in mind that $f\left(x\right)$ is well localized, we only take into account the overlap between the Wannier functions associated with the nearest-neighboring sites. By substituting Eq. (A9) into Eq. (2.5), after some straightforward algebra, we arrived at the energy per particle reading

$$\varepsilon\left(k\right)=\varepsilon_0-\tau\cos\left(kd\right) \tag{A10}$$

Here, ε_0 is the on-site energy and τ is the tunneling parameter. More specifically, we have calculated $\varepsilon_0=\frac{1}{2k_L}\int f\left(x\right)\left\{-\frac{1}{2}\frac{\partial^2}{\partial x^2}+v\cos\left(x\right)+\frac{1}{2}\left[c_1+c_2\cos\left(x\right)\right]df\left(x\right)^2\right\}f\left(x\right)dx$. Note that ε_0 depends on the parameters v, c_1 and c_2, but not on the wave number k. The tunneling parameter τ is given by

$$\tau=\frac{1}{2k_L}\int f\left(x\right)\left\{-\frac{1}{2}\frac{\partial^2}{\partial x^2}+v\cos\left(x\right)+\frac{1}{2}\left[c_1+c_2\cos\left(x\right)\right]df\left(x\right)^2\right\}f\left(x-d\right)dx \tag{A11}$$

We must point out that during the derivation of Eq. (A10), the term $\int f^2\left(x\right)f^2\left(x-d\right)dx$ was omitted, which for localized functions, turn out to be much smaller, whereas the term $\int f^3\left(x\right)f\left(x-d\right)dx$ was kept. Deep in tight-binding regime, the Wannier function $f\left(x\right)$ can be approximated by a Gaussian form $f\left(x\right)=\exp\left[-\left(x+\frac{d}{2}\right)^2/\left(2\sigma^2\right)\right]/\left(\pi^{1/4}\sqrt{\sigma}\right)$, where σ is the extension of the Gaussian which can be determined by minimizing the energy of the system. After straightforward calculations, the width σ and the inverse compressibility are derived as

$$\sigma\approx\frac{d}{2\pi V^{\frac{1}{4}}}\left(1+\frac{1}{16V^{\frac{1}{2}}}\right) \tag{A12}$$

$$\frac{1}{\kappa}\approx\frac{1}{\sqrt{2\pi}}\left(\frac{d}{\sigma}\right)\left(c_1-c_2e^{-\frac{\pi^2}{2}\left(\frac{\sigma}{d}\right)^2}\right) \tag{A13}$$

The effective mass can be obtained from a standard procedure [36], and here we present the final result

$$\frac{m}{m^*}=\left[\frac{1}{4}\left(\frac{d}{\sigma}\right)^4-\frac{1}{2}\left(\frac{d}{\sigma}\right)^2-8\pi^2Ve^{-\pi^2\left(\frac{\sigma}{d}\right)^2}-8\pi\sqrt{2\pi}c_1\left(\frac{d}{\sigma}\right)e^{-\frac{1}{8}\left(\frac{d}{\sigma}\right)^2}\right]e^{-\frac{1}{4}\left(\frac{d}{\sigma}\right)^2} \tag{A14}$$

With both the compressibility κ and the effective mass m^* being derived, we can readily calculate the sound speed in the tight-binding regime. Our analysis result is consistent with the numerical calculations (Fig. 2) in corresponding regimes, suggesting that the tight-binding treatment Eq. (A9) is a reliable method.

[1] C. Chin, R. Grimm, P. Julienne, E. Tiesinga, Rev. Mod. Phys. **82**, 1225 (2010)
[2] M. Theis, G. Thalhammer, K. Winkler, M. Hellwig, G. Ruff, R. Grimm, J.H. Denschlag, Phys. Rev. Lett. **93**, 123001 (2004)
[3] R. Qi, H. Zhai, Phys. Rev. Lett. **106**, 163201 (2011)
[4] R. Yamazaki, S. Taie, S. Sugawa, Y. Takahashi, Phys. Rev. Lett. **105**, 050405 (2010)
[5] I. Bloch, J. Dalibard, W. Zwerger, Rev. Mod. Phys. **80**, 885 (2008)
[6] G. Raithel et al., Phys. Rev. Lett. **78**, 630 (1997)
[7] T. Mller-Seydlitz et al., Phys. Rev. Lett. **78**, 1038 (1997)
[8] S.E. Hamann et al., Phys. Rev. Lett. **80**, 4149 (1998), and references therein
[9] S. Friebel, C. D'Andrea, J. Walz, M. Weitz, T.W. Häsch, Phys. Rev. A **57**, R20 (1998)
[10] M. Raizen, C. Salomon, Q. Niu, Phys. Today **50**, 30 (1997)
[11] L. Guidoni, P. Verkerk, Phys. Rev. A **57**, R1501 (1998). and references therein
[12] L. Guidoni, C. Triché, P. Verkerk, G. Grynberg, Phys. Rev. Lett. **79**, 3363 (1997)
[13] K.I. Petsas, A.B. Coates, G. Grynberg, Phys. Rev. A **50**, 5173 (1994)
[14] I.H. Deutsch, P.S. Jessen, Phys. Rev. A **57**, 1972 (1998)
[15] K. Berg-Søensen, K. Mømer, Phys. Rev. A **58**, 1480 (1998)
[16] D.I. Choi, Q. Niu, Phys. Rev. Lett. **82**, 2022 (1999)
[17] B.Wu, Q. Niu, Phys. Rev. A **64**, 061603(R) (2001)
[18] E.J. Mueller, Phys. Rev. A **66**, 063603 (2002)
[19] A. Polkovnikov, E. Altman, E. Demler, B. Halperin, and M.D. Lukin, Phys. Rev. A. **71**, 063613 (2005)
[20] V.I. Yukalov, Laser Phys. **19**, 1 (2009)
[21] O. Morsch, J.H. Müller, M. Cristiani, D. Ciampini, E. Arimondo, Phys. Rev. Lett. **87**, 140402 (2001)
[22] L. Fallani, L.D. Sarlo, J.E. Lye, M. Modugno, R. Saers, C. Fort, M. Inguscio, Phys. Rev. Lett. **93**, 140406 (2004)
[23] O. Morsch, M. Oberthaler, Rev. Mod. Phys. **78**, 179 (2006)
[24] S.L. Zhang, Z.W. Zhou, B. Wu, Phys. Rev. A **87**, 013633 (2013)
[25] J. Stenger, S. Inouye, A.P. Chikkatur, D.M. Stamper-Kurn, D.E. Pritchard,W. Ketterle, Phys. Rev. Lett. **82**, 4569 (1999)
[26] D.M. Stamper-Kurn, A.P. Chikkatur, A. Gölitz, S. Inouye, S. Gupta, D.E. Pritchard,W. Ketterle, Phys. Rev. Lett. **83**, 2876 (1999)
[27] J.M. Vogels, K. Xu, C. Raman, J.R. Abo-Shaeer, W. Ketterle, Phys. Rev. Lett. **88**, 060402 (2002)
[28] J. Steinhauer, R. Ozeri, N. Katz, N. Davidson, Phys. Rev. Lett. **88**, 120407 (2002)
[29] R. Ozeri, J. Steinhauer, N. Katz, N. Davidson, Phys. Rev. Lett. **88**, 220401 (2002)
[30] J. Steinhauer, N. Katz, R. Ozeri, N. Davidson, C. Tozzo, F. Dalfovo, Phys. Rev. Lett. **90**, 060404 (2003)
[31] X. Du, S. Wan, E. Yesilada, C. Ryu, D.J. Heinzen, Z. Liang, B. Wu, New. J. Phys. **12**, 083025 (2010)
[32] M. Kräer, C. Menotti, L. Pitaevskii, S. Stringari, Eur. Phys. J. D **27**, 247 (2003)
[33] C. Menotti, M. Kräer, L. Pitaevskii, S. Stringari, Phys. Rev. A **67**, 053609 (2003)
[34] Y. Hu, Z.X. Liang, Phys. Rev. Lett. **107**, 110401 (2011)
[35] Y. Hu, Z.X. Liang, Mod. Phys. Lett. B **27**, 1330010 (2013)
[36] Z.X. Liang, X. Dong, Z.D. Zhang, B. Wu, Phys. Rev. A **78**, 023622 (2008)
[37] D. Pines, P. Noziéres, *The Theory of Quantum Liquids*, vol. I (Benjamin, New York, 1966)
[38] P. Noziéres, D. Pines, *The Theory of Quatum Liquids*, vol. II (Addison-Wesley, Reading, 1990)
[39] E. Taylor, E. Zaremba, Phys. Rev. A **68**, 053611 (2003)
[40] D. Boers, C. Weiss, M. Holthaus, Europhys. Lett. **67**, 887 (2004)
[41] R. Ozeri, N. Katz, J. Steinhauer, N. Davidson, Rev. Mod. Phys. **77**, 187 (2005)